Beam duct for the 1 MW neutral beam injector on TCV

Matthieu Toussaint[a], Stefano Coda[a], Frédéric Dolizy[a], Basil Duval[a], Alexander Nicola Karpushov[a], Yves Martin[a], Roberto Maurizio[a] and the TCV team[a]

[a]*Ecole Polytechnique Fédérale de Lausanne (EPFL), Swiss Plasma Center (SPC), CH-1015 Lausanne, Switzerland*

The 1MW power of the neutral beam injector (NBI) enters the plasma of the Tokamak à Configuration Variable (TCV) through a duct. The original beam propagation model predicted a maximal heat flux on the internal faces of the duct below 350 kW/m^2, leading to an acceptable temperature rise for the 2s nominal pulse duration. During commissioning, the NBI showed unacceptable overheating in the duct, the beam divergence being higher than expected. Several ion source grids have been tested to mitigate the beam divergence however the overheating of the duct is still problematic. Since then, the NBI operates with reduced power and duration to avoid damaging the beam duct.

This paper describes the design and thermal analysis of a new beam duct capable of withstanding NBI shots at nominal regime for a range of modeled neutral beam divergences. The design drivers are the high heat flux protection and the accumulated heat dissipation. The concept features a thermal shield composed of a smooth elliptical castellated layer surrounded by an actively cooled structure.

Keywords: TCV, Neutral Beam Heating Injector, Duct, Cooling, Thermal

1. Introduction

The TCV has undergone a major upgrade including the installation of a 1MW NBI [1, 2]. For efficient plasma heating the beam is transmitted in the TCV vacuum vessel (VV) through a duct oriented tangentially relative to the plasma axis. The duct is composed of a rectangular port welded to the VV with aperture 170x220mm and a conical extension for the connection to the circular NBI outlet of aperture Ø250mm (fig.1). The position z=0 corresponds to the position of the ion optical system (IOS) of the NBI.

1. Neutral Beam Injector
2. Extension (part of beam duct)
3. Port (part of beam duct)
4. TCV vacuum vessel
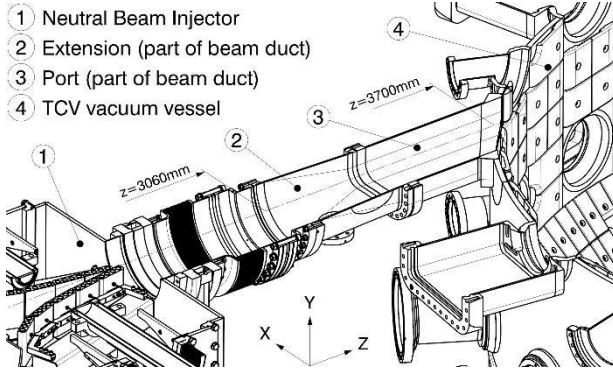
z=3700mm

z=3060mm

Fig. 1. Horizontal cut of the concerned region.

A nominal regime of 1 MW power for 2 seconds every 12 minutes is expected. A beam propagation model [3] was used for preliminary thermal simulations, with expected main parameters as follows:

- Circular grids aperture = Ø250mm.
- Vertical angular divergence $\delta\alpha_{\parallel}$ = 12 mrad.
- Horizontal angular divergence $\delta\alpha_{\perp}$ = 20 mrad.
- Optimal focal distance of the grid system = 3600mm

The predicted beam power density profile was divergent along the beam axis z in the duct region (fig.2). The incidence angle of ~1.3° with the beam axis led the most exposed faces of the extension to an average effective heat flux of ~300 kW/m^2. A maximal temperature elevation of ~40°C ensuing a shot at nominal regime was expected very locally on the lateral faces of the extension, which are the most exposed. Subsequently, most of the faces were expected to remain at room temperature. No thermal protection nor active cooling of the duct was therefore envisioned.
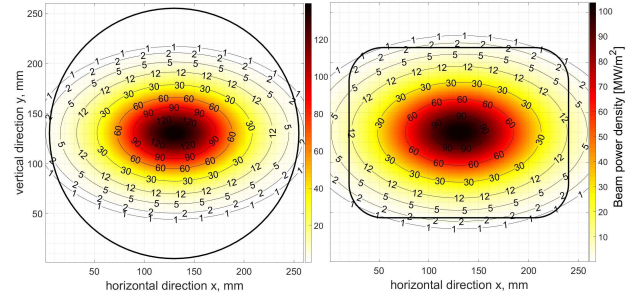

Fig. 2. Expected beam profile at duct entrance (z=3060mm, left) and at duct outlet (z=3700mm, right). Circle represents Ø250mm, rectangle represents 170x220mm.

However, the commissioning of the NBI (2016) showed high overheating of the extension. Thermocouples measurements showed that maximal elevation temperature on the inner faces of the duct was ~500°C per shot at nominal regime. Related to this observation, a device developed at SPC was used to estimate the real beam power density profile along the z axis in the duct region. Aspect ratio of the measured beam profile largely differed from the contractual one, being 35x8mrad instead of 20x12mrad, confirming the overheating observation. Limitation of the NBI power and duration was a direct consequence of it. Since then, new sets of grids have been subcontracted to mitigate the beam divergence. The two first sets (2017 and 2018) did not show significant improvement, while the last set of

grids (2019) produced a beam with an improved divergence of 24x10mrad. Considering the severe operational restrictions of the NBI since its commissioning and the difficulty to produce grids with expected divergence, a new beam duct design is proposed to allow NBI operation at nominal regime and is described hereunder.

2. Design

2.1 Description of the new extension

The main design drivers being the high heat flux protection and the stored heat dissipation, the system shall also not exceed the current external dimensions due to the severe lack of space in the surroundings.

First thermal considerations indicated that the geometrical transition from circle Ø250mm to rectangle 170x220mm should features smooth faces with incident angle as low as possible. The proposed beam duct features tiles forming an elliptical transition (fig.3), minimizing the incident angle as the power density increases. This layer of tiles constitutes the high heat flux shielding and is castellated to avoid potential internal damages caused by important temperature gradients. It also permits tiles replacement in case of heat damage, erosion damage or maintenance operation. Thermocouples are integrated in dedicated tiles for temperature control.
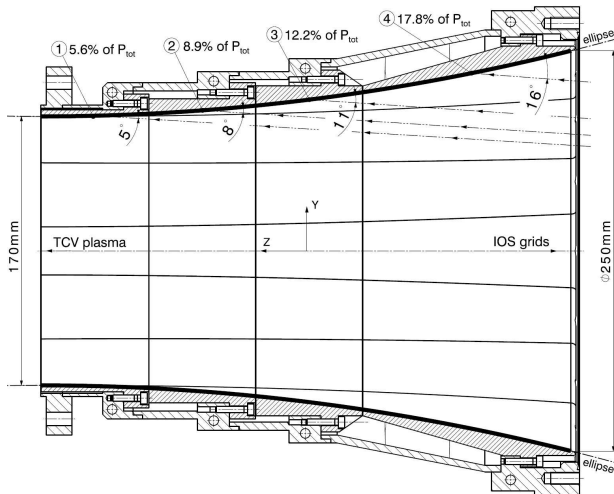
Fig. 3. Vertical section of elliptical transition showing beam particles lines and incidence angles. Correspondent fraction of deposited power is indicated.

The proposed shape provides a significant decrease of ~25% of the maximal heat flux deposited on the internal surface of the extension compared to the classic shape currently installed (fig. 4). The smoothness of the first layer prevents any perpendicular exposition to the beam particle lines, being a key point to avoid hot spots. Such a continuous surface is rendered possible due to the hidden fixation screws (fig.5).
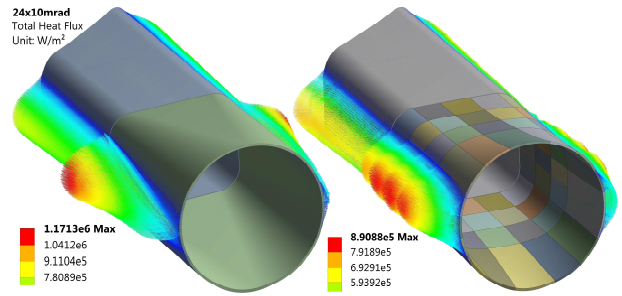
Fig. 4. Maximal heat flux comparison between the classic shape and the new design, 24x10mrad divergence.
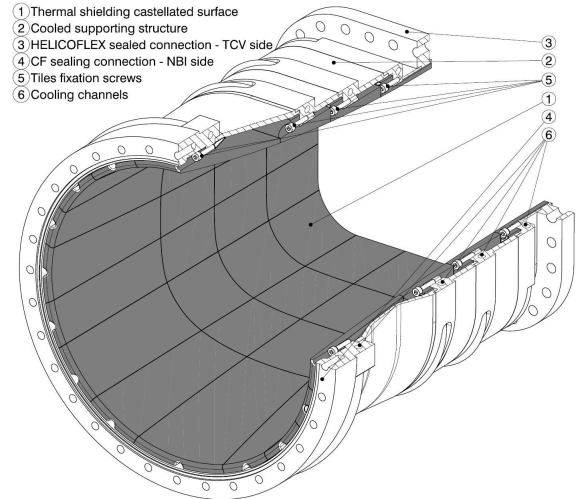
Fig. 5. Elliptical swept surface transition, forming the thermal shielding.

For plasma pollution reasons, the material of the first layer can be either graphite R6650 or metal (CuCrZr or 316LN) with a boron carbide deposition. Whatever the chosen material, the proposed design permits a simple manufacture starting from 4 single blocs and then dividing them finely by electro-discharge machining. The tiles are fixed on the actively cooled supporting structure (stainless steel 316LN), composed of 6 welded elements (fig.6). This segmentation is necessary for tooling access to create the hidden threaded holes for tiles fixation, while permitting simple CNC 3 axis machining and avoiding bulky raw material procurement. Each segment comprises a surrounding cooling channel which serves dissipating the thermal energy accumulated in the tiles after every NBI pulse.
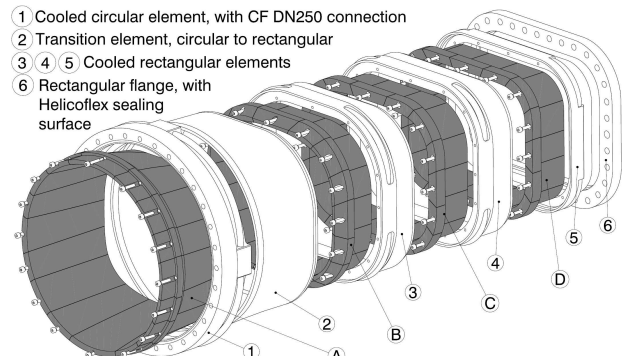
Fig. 6. Segments of the cooled supporting structure (1-6) and blocs of the thermal shielding layer (A-D).

2.2 Description of the cooled port

The port is welded to the TCV VV and can therefore not be modified. Moreover, the lack of available space around it prevents the installation of a consequent cooling system. To avoid thermal ratcheting, the port has been covered with 7 plates made out of copper EN CW004A and actively cooled (fig.7). The thermal contact is enhanced by both tightening cables and a soft thermal conductive graphite layer placed between the copper plates and the port. Thermocouples are integrated to measure the outer surface temperature of the port.
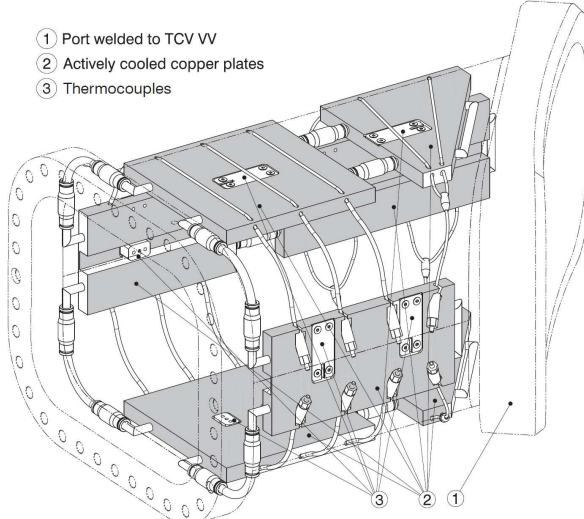

① Port welded to TCV VV
② Actively cooled copper plates
③ Thermocouples

Fig. 7. Port welded to TCV VV equipped with actively cooled copper plates.

3. Thermo-mechanical analysis

The whole beam duct (extension and port) is analyzed by Finite Element Method (FEM) for 3 different beam divergences and 3 materials of tiles. The keypoints of the analysis are the maximal temperature ensuing a pulse at nominal regime (t = 2s) as well as succeeding the cooling phase (t = 722s). Thermomechanical stresses and thermal ratcheting along the day are equally computed.

3.1 Boundaries conditions and assumptions

ANSYS thermal transient module was used. 3D distributed heat fluxes of the 3 considered beams were imported as clouds of points from the beam numerical model. The load was imported in a FEM analysis and applied on perpendicular targets placed at z=3060mm and at z=3700mm for 2s. Total power in the range 0.97-1.13 MW was computed for all the cases, validating the imported heat flux.

Tiles in stainless steel 316LN, CuCrZr and graphite R6650 were considered. Port cooling plates are computed with copper EN CW004A and the rest of the supporting structure with stainless steel 316LN. All the materials are considered with temperature dependencies for the density, the thermal conductivity and the specific heat.

Different areas of thermal contact between the tiles and the supporting structure were considered, the graphite tiles being held with 1 fixation screw to allow free stress thermal expansion, while the 316LN or CuCrZr tiles being held with 3 fixation screws (same thermal expansion coefficient). Contact of type bonded was assumed under the screw head region. For the copper plates installed around the port, a reduced contact area representing the tightening cables contact region was considered. An interlayer of 0.1mm thick and conduction coefficient 9 W/mK was considered to simulate the thermal conductive graphite interlayer.

Active cooling inside the cooling channels of the copper plates and the extension runs permanently. Heat transfer coefficients from 3'000 to 10'000 W/m²K were approximated analytically. Effect of these coefficients was analyzed by FEM for values 1000, 5000 and 10'000 W/m²K and led to a negligible difference <1.5°C at the end of the cooling phase. Thus a mean value of 5000 W/m²K was retained.

Natural convective cooling also exists in regions of the duct which are not covered by Microtherm insulation layers. Typical heat transfer coefficient of 5 W/m²K was analyzed by FEM and resulted in a <0.5°C difference ensuing the cooling phase, active cooling being predominant. Natural convective cooling was therefore neglected.

Thermal radiation was neglected as well due to marginal effect. Emissivity coefficient of 1.0 for graphite and 0.1 for polished stainless steel or copper were computed and led to a difference <1°C on the maximal temperature at t=2s and t=722s.

3.2 Results

The first important result to notice is a maximal temperature on the internal surfaces of the non-protected port below 200°C ensuing a 2 second pulse with the last set of grids (fig. 8). When considering thermal ratcheting along an intensive day of 40 NBI pulses, this temperature is converging towards an asymptote of ~200°C (fig.10). These values are in the range of the VV baking temperature (thermocouples placed on the VV surface measures 220°C to 240°C) and are therefore acceptable for those non protected surfaces.

The second crucial result is the temperature of the first protection layer. For 1 thermal cycle, graphite and CuCrZr are suitable with the last set of grids installed at TCV while 316LN is close to 250°C (fig. 9). Thermal ratcheting over an intensive day of 40 NBI pulses generates a maximal temperature of ~200°C for CuCrZr, ~227°C for graphite and close to 300°C for 316LN.

Analytical approximations show that maximal thermomechanical stresses are marginal for replaceable CuCrZr or graphite tiles of the first protection layer, validating the castellated design. While never exceeding 200°C with the last set of grids, the port is subject to higher stresses, locally exceeding the elasticity limit. Those stresses are locally spotted and are due to the rapid surface temperature increase, generating a considerable thermal gradient in the low thermal conductive stainless steel 316LN.
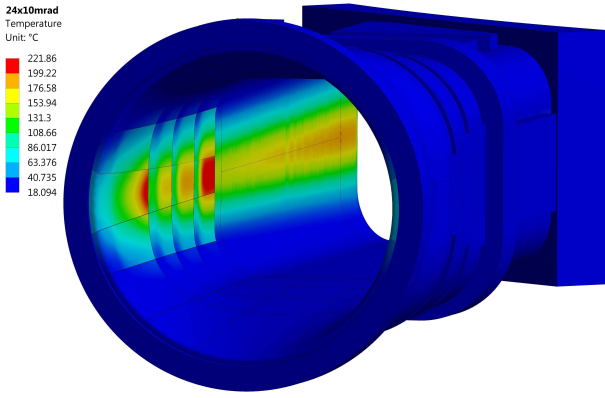
Fig. 8. Surface temperature of duct ensuing a 2s pulse, graphite tiles with 24x10mrad beam display.
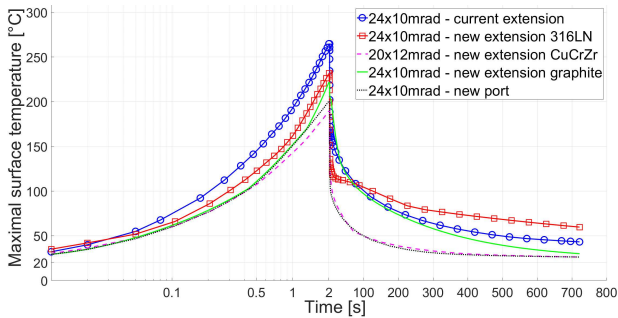

Fig. 9. Maximal surface temperature for different materials and divergences. The initial cycle is displayed.
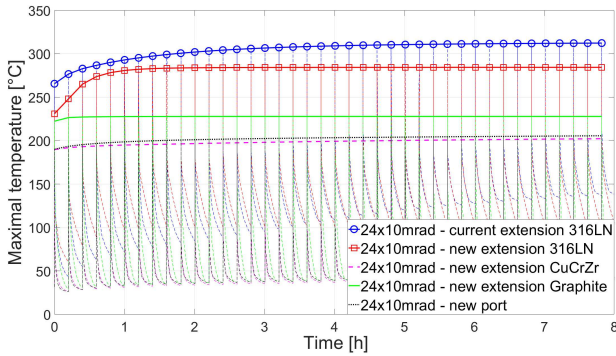

Fig. 10. Thermal ratcheting effect over a day of operation. 40 cycles are displayed. Curves are interpolated between each maximum temperature of each cycle.

4. Conclusion and outlook

Considering the last set of grids with beam divergence of 24x10mrad, the paper shows that the proposed shape of the beam duct extension provides a significant decrease of ~25% of the maximal heat flux on the internal faces. Different materials are proposed for the first protection layer of the beam duct extension, the most adapted being the CuCrZr coated with boron carbide. Due to its good thermal conductivity, maximal temperature on CuCrZr tiles never exceeded 200°C while cooling time was the quickest. Feasibility of boron carbide deposition on CuCrZr is still to be assessed. At a higher cost and with a slower cooling time due to the reduced thermal contact area (1/3), first protection layer in graphite is equally suitable, without requiring boron carbide coating. On the other hand, tiles in 316LN should not be used as a long term solution as peak temperatures close to 300°C were computed and could lead to thermal fatigue cracks. Cooling time of tiles in 316LN is equally problematic. 316 LN was considered because it easily allows a boron carbide coating.

Temperatures computed on the internal faces of the non-protected port never exceeded 200°C, being lower than the baking temperature of the VV. The port external cooling device was installed with success in summer 2019 (fig.11) and for limited NBI pulses, thermocouples showed a thermal behavior in accordance with numerical expectations.

Thermomechanical stresses were negligible in the CuCrZr or graphite replaceable tiles of the first protection layer, castellated design being a key point. However, thermomechanical stresses in the non-castellated port are much higher and have to be taken into consideration as they could play a significant role in the lifetime of the port. Indeed, thermo-mechanical stresses are exceeding locally the elastic limit of the port made of stainless steel 316LN. Further thermal elasto-plastic analysis is required to identify any potential fatal issue. Protection of the internal faces of the port from intense temperature gradients could be required.

To conclude, temperature control of the beam duct during the entire lifetime of the NBI is essential for the integrity of the TCV VV. It is even more relevant when considering that the beam parameters may change over time, as already observed in the past.
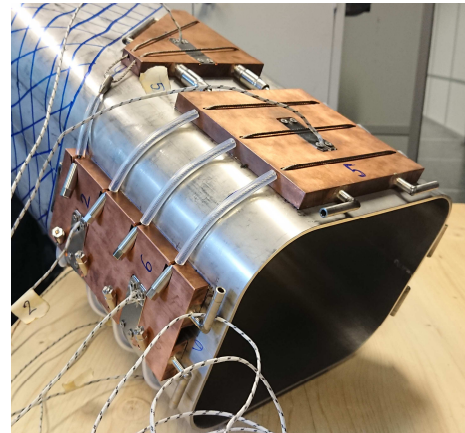

Fig. 11. Mockup of the installation of the port cooling system.

References

[1] A. Fasoli for the TCV team, TCV Heating and In-Vessel Upgrades for Addressing DEMO Physics Issues, Nuclear Fusion 55 (2015) 043006 .

[2] A.N.Karpushov, et al.; Neutral beam heating on the TCV tokamak; Fusion Engineering and Design (2017); In Press; DOI:10.1016/j.fusengdes.2017.02.076

[3] Akhmetov,T.D.; Davydenko,V.I.; Ivanov,A.A.; Model of neutral-beam propagation in a duct with scrapers; IEEE Trans. Plasma Sci. (USA), v.36, n.4, Aug. 2008, p.1545-51; DOI:10.1109/TPS.2008.917951